

## Aperture measurements with ac dipoles and movable collimators in the Large Hadron Collider

N. Fuster-Martínez\*

*Instituto de Física Corpuscular (CSIC-UV), 46908 Valencia, Spain and CERN, 1211 Geneva, Switzerland*

R. Bruce, M. Hofer, T. Persson, S. Redaelli, and R. Tomás

*CERN, 1211 Geneva, Switzerland*



(Received 11 February 2022; accepted 26 September 2022; published 19 October 2022)

This paper presents a first experimental demonstration of a new nondestructive method for aperture measurements based on ac dipoles. In high intensity particle colliders, such as the CERN Large Hadron Collider (LHC), aperture measurements are crucial for a safe operation while optimizing the optics in order to reduce the size of the colliding beams and hence increase the luminosity. In the LHC, this type of measurements became mandatory during beam commissioning and the current method used is based on the destructive blowup of bunches using a transverse damper. The new method presented in this paper uses the ac-dipole excitation to generate adiabatic forced oscillations of the beam in order to create losses to identify the smallest aperture in the machine without blowing up the beam emittance. A precise and tuneable control of the oscillation amplitude enables the beams to be reused for several aperture measurements, as well as for other subsequent commissioning activities. Measurements performed with the new method are presented and compared with the current LHC transverse damper method for two different beam energies and two different operational optics.

DOI: [10.1103/PhysRevAccelBeams.25.101002](https://doi.org/10.1103/PhysRevAccelBeams.25.101002)

### I. INTRODUCTION

In most storage rings, detailed knowledge of the geometric aperture is required in order to guarantee sufficient beam clearance, safe operation, and the minimum activation of accelerator equipment due to beam losses. In the CERN Large Hadron Collider (LHC) [1], where proton and heavy-ion beams are brought into collision for high-energy physics experiments, the control of the available aperture is extremely critical to achieve the nominal stored proton beam energy of 362 MJ in a superconducting (SC) accelerator environment. Even small losses can cause the SC magnets to quench, changing their state from superconducting to normal conducting or in extreme cases lead to material damage that can be very costly to repair in terms of both time and money.

In this paper, we use the term aperture to define the *normalized* machine aperture  $A_{x,y}$  at any given longitudinal location. It is defined as the smallest transverse distance in the horizontal and vertical planes,  $r_{x,y}$ , between the beam

center and the mechanical aperture, expressed in units of the local beam size,  $\sigma_{x,y}$ :

$$A_{x,y}(s) = r_{x,y}(s)/\sigma_{x,y}(s), \quad (1)$$

where the beam size depends on the Twiss  $\beta$ -function as

$$\sigma_{x,y}(s) = \sqrt{\frac{\beta_{x,y}\epsilon_n^{\text{design}}}{\beta_{\text{rel}}\gamma_{\text{rel}}}}. \quad (2)$$

Note that here we include the design value of the normalized emittance,  $\epsilon_n^{\text{design}}$ , with  $\beta_{\text{rel}}$  and  $\gamma_{\text{rel}}$  as the relativistic factors. The design emittance is used in order to more easily relate the aperture to the machine protection system settings and do comparisons between different LHC runs or fills. The aperture expressed in real beam  $\sigma$  could thus be different and can vary between fills and even between different bunches in the same fill. However, the settings of the collimators, in units of  $\sigma$ , vary by the same scaling factor, such that the relative protection of the machine aperture is unaffected. Note that the ideal aperture is reduced by a number of imperfections and tolerances, for example, misalignment of magnets and vacuum pipes, orbit errors within machine elements and off-energy offsets.

This normalized aperture is directly connected to the risk of local beam losses that could potentially limit the accelerator performance. In particular, the performance

\*nuria.fuster@ific.uv.es

Published by the American Physical Society under the terms of the [Creative Commons Attribution 4.0 International license](https://creativecommons.org/licenses/by/4.0/). Further distribution of this work must maintain attribution to the author(s) and the published article's title, journal citation, and DOI.

TABLE I. Measured and predicted bottleneck aperture values for the 2017 top energy LHC optics for both beams and planes. The predicted values had been computed without and with measured tolerances [4].

Beam	Plane	$A_{\text{without tol}}^{\text{predicted}} (\sigma)$	$A_{\text{with tol}}^{\text{predicted}} (\sigma)$	$A^{\text{measured}} (\sigma)$
1	H	11.5	9.2	$10.6 \pm 0.5$
1	V	11.5	9.2	$11.1 \pm 0.5$
2	H	11.5	9.2	$10.9 \pm 0.5$
2	V	11.5	9.2	$10.5 \pm 0.5$

reach in a collider depends on the available normalized aperture in the final-focus system [2,3]. The triplet quadrupole magnets, used to focus the beams at the interaction point (IP), typically represent the locations with the smallest aperture in the machine, known as the aperture bottleneck.

At the LHC, for colliding-beam operations and  $\beta^*$  values below about 5 m,<sup>1</sup> the bottleneck locations were consistently measured during Run 1 (2010–2013) and Run 2 (2015–2018) at the inner triplets in the high luminosity experiments in the interaction regions (IRs) 1 and 5 [4], where the smallest  $\beta^*$  is deployed for proton runs. These observations are consistent with the expectations from calculations performed using the numerical algorithm implemented in the MAD-X aperture module, described in detail in Refs. [1,5–7], which computes the smallest transverse distance, normalized by the local transverse beam size, between the closed orbit and the physical aperture. The MAD-X algorithm takes into account aperture, orbit, and optics tolerances. Note that these calculations are limited by the fact that many tolerances were unknown at the design phase. During the LHC Run 1, several tolerances affecting the aperture model were found to be less restrictive than in the worst-case scenarios assumed during the design phase of the LHC. This was the case for the orbit control, optics correction, and the alignment of some machine elements, to name a few. The agreement between expectations and measurements was improved from  $2\sigma$ , with design tolerances, to  $0.5\text{--}1.5\sigma$  with measured tolerances [4]. Table I presents an example of predicted and measured bottleneck aperture values for the 2017 top energy optics. The predicted values had been calculated without and with measured tolerances [4].

Decreasing  $\beta^*$  causes a decrease in available triplet aperture. The settings of the LHC multistage collimation system [2], designed to protect the LHC from normal and abnormal losses, define the smallest normalized aperture that can be protected and therefore imposes limitations also on the smallest achievable  $\beta^*$ , which translates into limits on the achievable luminosity, in both operations with protons [3] and heavy ions [8,9].

<sup>1</sup>In LHC operation so far, the optical function  $\beta^*$  is identical in both transverse planes.

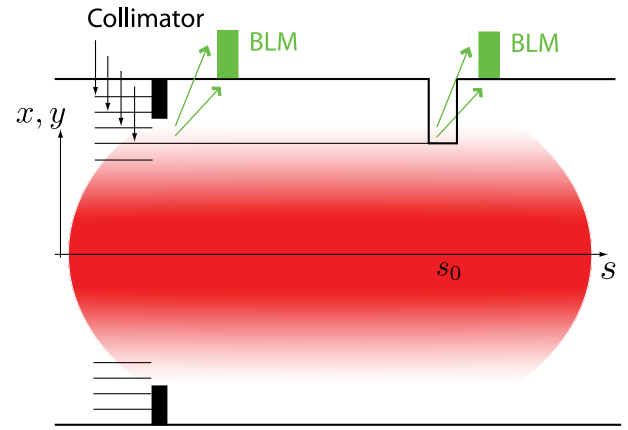


FIG. 1. Collimator scan with transverse damper beam blowup technique illustration. The reference collimator is indicated in black and the BLMs in green. Note that in this example, five collimator steps were performed spaced about a given fraction of  $\sigma$ . Reprinted under CC BY 4.0 license from paper [4].

Many beam-based aperture measurement techniques were developed for precise measurements during the LHC Run 1 and Run 2 [4] operations. All the techniques developed are based on generating beam losses either by shifting the beam orbit or by blowing up its emittance and monitoring them using about 4000 beam loss monitors (BLMs) installed around the ring [10,11]. The BLMs allow us to measure local losses at most elements and identify the bottleneck locations. Different strategies are then used to reconstruct the available aperture in units of beam size,  $\sigma$ . The standard LHC aperture measurement technique used during the Run 2 LHC operation consists of performing a gentle blowup of one low-intensity bunch using white-noise excitation from a transverse damper system until losses are measured at a reference collimator, as illustrated in Fig. 1. Once losses are localized at the reference collimator, the gap of this collimator is opened in steps of  $0.5\sigma$  until the losses move from this collimator to the bottleneck location. The detailed experimental and analysis procedures can be found in Ref. [12]. Note that, in order not to interfere with the measurements, all other collimators in the machine need to be more open than the reference collimator and the aperture bottleneck during the scan. Usually, some selected collimators have to be kept within a certain margin to the reference collimator for protection reasons, while all others are fully retracted. This method can only be used with low-intensity bunches because of the high level of losses generated, allowing just one measurement before the bunches become unusable for other activities.

During the LHC Run 2 operation, aperture measurements became mandatory as part of the yearly LHC beam commissioning to verify that the minimum aperture in the machine is under control and protected by the collimation system. The LHC beam commissioning is performed after

long (2–3 years) or medium (few months) periods without operation and includes many different activities to validate the machine operation. First, using low-intensity beams, machine protection activities such as collimators alignment and settings validation have to be performed, as well as optics measurements and corrections [13]. Once the machine protection is setup and the final orbit deployed, the machine configuration is validated by analyzing controlled beam losses in both transverse planes, off-momentum losses, and losses due to synchronization failures of the dump kickers. The full beam commissioning takes about 1 month. A continuous effort is being made to improve the efficiency of the beam commissioning strategy and reduce the time required while keeping the same level of protection.

ac dipoles are dipole magnets that can be adiabatically turned on and off repeatedly to excite driven oscillations of the beam while preserving the beam emittance [14–16]. They have been used in synchrotrons for a variety of applications [17] such as avoiding spin resonances in the Brookhaven Alternating Gradient Synchrotron (AGS) [18] and later for the first time to measure linear optics functions in the Brookhaven Relativistic Heavy Ion Collider (RHIC) [19] and in the Fermilab circular accelerator Tevatron [20]. Currently, ac dipole is the single most important tool for optics measurements in the LHC and the High-Luminosity LHC, as well as a key element for new linear and nonlinear correction techniques [21–24]. This is in part due to the fact that large single kicks are not allowed when the machine is being operated at its maximum energy, because of machine protection considerations. Furthermore, new applications of the ac dipoles have been developed thanks to their proven reliability, such as amplitude detuning measurements in the presence of head-on beam-beam interactions [25], machine impedance measurements [26], and beam cooling [27,28]. Other facilities are now also using ac dipole excitations for optics measurements such as ESRF [29], PETRA III [30,31], SuperKEKB [32], and ALBA [33].

This paper presents the first experimental demonstration of aperture measurements using ac dipole excitations combined with a reference collimator scan procedure. These measurements aim to determine the corresponding aperture in units of beam size,  $\sigma$ , in order to set the machine protection settings. The main advantage of the ac-dipole method, with respect to the transverse damper method currently used at the LHC [4], is the fact of being nondestructive, enabling the beams to be subsequently reused for other activities that offer the possibility to improve the beam commissioning efficiency. In addition, some optics measurements such as amplitude detuning [22] and resonance driving term measurements could benefit from an adjacent quick nondestructive aperture measurement in order to be performed with the highest possible safe excitation amplitude, hence improving their precision.

Section II summarizes the main elements required to understand the aperture measurement experiments at the LHC. In Sec. III, the new ac-dipole method is described in detail and the results of the first tracking simulations performed to evaluate its feasibility are presented. Section IV describes the first aperture measurements performed combining an ac dipole and a movable collimator, for two different beam energies and two different optics configurations. The agreement with the transverse damper method is discussed in Sec. V.

## II. BASELINE APERTURE MEASUREMENTS METHOD

Four out of the eight LHC IRs are dedicated to particle physics experiments, which are ATLAS, ALICE, CMS, and LHCb at IR1, IR2, IR5, and IR8, respectively. In these IRs, the two counterrotating LHC beams, Beam 1 and Beam 2, collide. In order to refer to a particular quadrupole the name is composed of a number identifying the position with respect to the IP (1 being the closest), a letter [left (L) or right (R)] identifying the side with respect to the IP, and a number defining the corresponding IR. Figure 2 illustrates the case of the right side of IR5. In this figure, the layout until the ninth quadrupole from the IP is depicted, in which the main quadrupoles (Q) and dipoles (MB) are indicated. The triplet magnets correspond to Q1R5, Q2R5, and Q3R5. In addition, in Fig. 2, the corresponding horizontal and vertical closed orbit and  $\beta$  functions are illustrated as an example of the 2018 physics configuration optics with  $\beta_{x,y}^* = 25$  cm. In this plot, one can see how the  $\beta$  functions increase significantly in the triplet magnets before the IP.

The LHC collimation system is a multistage system organized in a well-defined transverse hierarchy, as illustrated in Fig 3, with different collimator families where each individual collimator consists of two movable jaws with the beam passing through the center. In the LHC, there

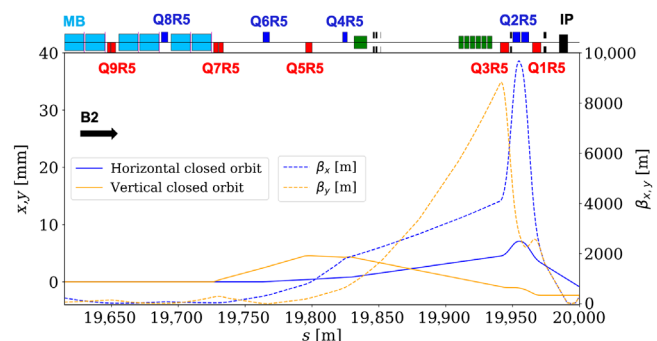


FIG. 2. Schematic layout of a section of IR5 with the main focusing (blue) and defocusing (red) quadrupoles and dipoles (light blue), from the IP to Q9, with the horizontal and the vertical closed orbit and  $\beta$  functions for the 2018 physics configuration optics with  $\beta_{x,y}^* = 25$  cm. Note here that the triplet quadrupoles of the final-focus system correspond to Q1R5, Q2R5, and Q3R5.

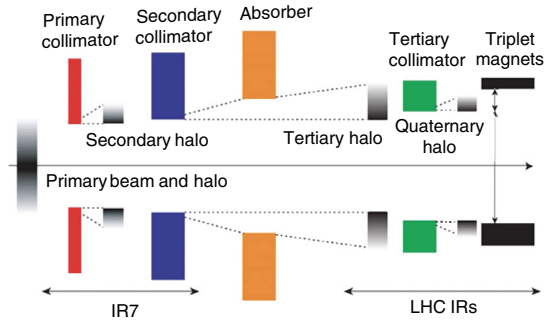


FIG. 3. LHC multistage collimation system scheme where the different collimator families are indicated [38].

are dedicated IRs for betatron and off-momentum cleaning, IR7 and IR3, respectively. There are then additional collimators at each IR hosting a physics experiment to provide further protection. The primary collimators (TCPs) in IR7 and IR3, made of carbon-fiber composite, which are the closest collimators to the beams, are typically used for aperture measurements. However, the tertiary collimators (TCTs) located upstream of the particle physics experiments in IR1, IR2, IR5, and IR8 are also exploited. The TCTs are made of Inermet-180 and aim to absorb the tertiary betatron beam halo and provide passive protection of the aperture bottlenecks in the triplet of the final-focus system, as well as a good control of the experimental backgrounds [34,35]. Other collimators are installed downstream of the experiments to absorb the debris from the collisions and to protect the machine in case of beam dump accidents, during which miskicked beams risk causing damage to sensitive elements [2,3,36,37]. All these collimators are installed in both beam 1 and beam 2 beamlines.

### III. AC-DIPOLE EXCITATIONS FOR APERTURE MEASUREMENTS

In this section, the method for aperture measurements using an ac dipole and the data analysis procedure are presented, along with the results of the first tracking simulations performed in order to validate the feasibility of the method. The simulation results are compared with the calculated aperture values obtained using the aperture module in the MAD-X accelerator design code.

#### A. ac-dipole aperture measurements method

The aperture measurement method using ac-dipole excitations and movable collimators presented in this paper follows a similar procedure as the standard LHC technique described in the introduction section of this paper, but instead of using the transverse damper system to generate losses, the ac dipole is used.

Using the ac dipole, large coherent beam oscillations are excited until losses are observed by the BLM system at the bottleneck location. The slow adiabatic ramp-up of the ac-dipole excitation allows for a continuous monitoring of

losses and enough time to safely trigger a beam dump before losses get too high. Since the emittance is preserved, multiple excitations of the same bunch can be repeatedly performed without degrading the beam quality. This is true as long as the nonlinear machine errors are not significant [39]. The machine setup, therefore, has to be chosen such that beam degradation due to nonlinearities is minimal. In order to do that, the octupoles are switched off during the measurements and the coupling is optimized. After the bottleneck location is identified, a reference collimator scan is performed, as illustrated in Fig. 1. For each reference collimator step, the beam is excited with the ac dipole. During the collimator scan, the beam loss rates are measured with the BLM system at the bottleneck locations in the ring  $R_{\text{loss}}^{\text{ring}}$  and at the reference collimator,  $R_{\text{loss}}^{\text{coll}}$  for different values of the collimator half-gap,  $A_{x,y}$ . An example is shown in Fig. 4 for an aperture measurement performed with the ac-dipole method in 2017 in the horizontal plane at injection energy and optics. In this plot, one can see the raw BLM signal at the bottlenecks Q6R2 (red) and Q4L6 (blue) and at the reference collimator (black), the horizontal ac-dipole kick being applied in each step of the scan in mm, and the reference collimator half-gap,  $A_x$ , in units of beam size. Note that during these measurements, synchronized with the ac-dipole excitation, losses were only observed at Q6R2, Q4L6, and at the reference collimator.

Because of the unavoidable intensity loss during the measurements, the raw BLM data are normalized by the number of protons lost as measured by the beam current

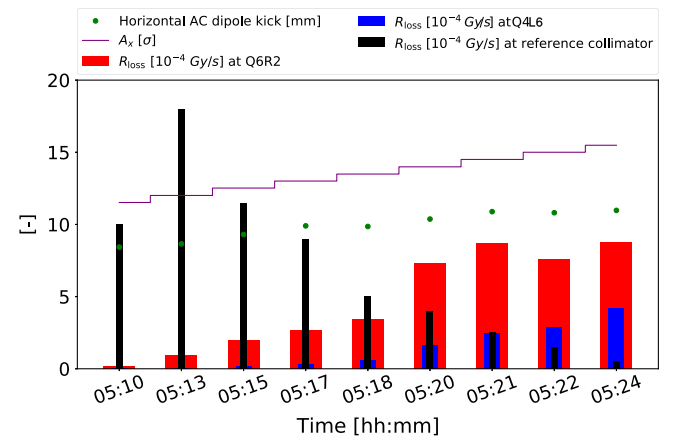


FIG. 4. Raw BLM signal at the bottlenecks Q6R2 (red) and Q4L6 (blue) and at the reference collimator (black), horizontal ac-dipole kick being applied in mm (green) and reference collimator half-gap in units of beam size from aperture measurements performed in 2017 at the LHC injection energy of 450 GeV. The measured aperture value of the bottlenecks is  $12.7\sigma$  for Q4L6 and  $12.9\sigma$  for Q6R2. Note that during these measurements, synchronized with the ac-dipole excitation, losses were only observed at Q6R2, Q4L6, and at the reference collimator. Adapted under CC BY 4.0 license from [40].

transformer. In addition, different optical functions, geometries, and materials can cause significant differences between the BLM signals at different locations in the machine. Because of that, each BLM signal is also normalized by its maximum measured value during the scan. This approach to data analysis was first introduced in [12]. An example of the resulting normalized loss rate,  $\tilde{R}_{\text{loss}}$ , as a function of the reference collimator half-gap is plotted in Fig. 5 for the data in Fig. 4. The loss rate at the reference collimator (black) and at the two identified bottlenecks (red and blue) is shown. The aperture value of the bottleneck corresponds to the intersection of the reference collimator half-gap and bottleneck curves corresponding in this example to  $12.7\sigma$  for Q4L6 and  $12.9\sigma$  for Q6R2. Note that during these aperture measurements at the injection optics configuration, losses were observed at two different locations in the machine in IR2 and IR6 indicating a very close aperture value at these two machine elements.

For these measurements, there are two important parameters to control in the setup of the ac dipole. The first is the amplitude of the oscillation,  $A_{x,y}^{\text{ac}}$ . This parameter has to be large enough for the beam to touch the aperture of the bottleneck but not too large to lose the beam by exceeding the BLM thresholds. The second is the ac dipole driving frequency, given by  $\nu_{x,y}^d$  which is defined as the ratio between the frequency of the ac dipole and the beam revolution frequency. If the difference,  $\delta_{x,y}^d$ , between  $\nu_{x,y}^d$  and the machine tune is too small, it can cause losses due to the finite frequency spread of the beam. In addition, if not chosen properly, the driving tunes can cross resonances causing beam losses that will interfere with the measurements [41]. Finally, if the  $\delta_{x,y}^d$  is too large, the horizontal and vertical ac-dipole induced  $\beta$  beating [19] increases,

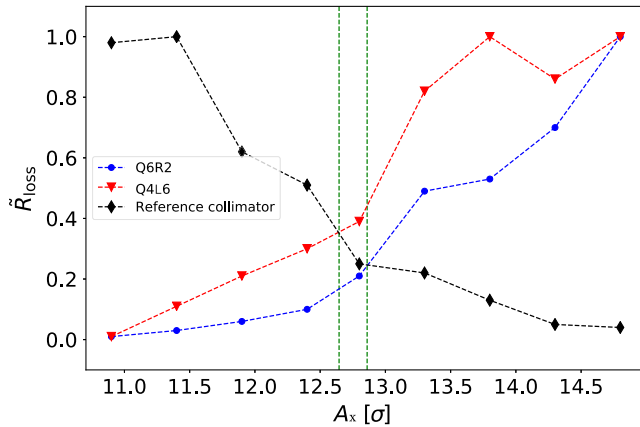


FIG. 5. Normalized losses at the reference collimator (black) and at the magnets Q6R2 (blue) and Q4R6 (red) as a function of the reference collimator half-gap,  $A_x$ , from aperture measurements performed with an ac dipole in 2017 at the LHC injection energy of 450 GeV. The measured aperture value of the bottlenecks corresponds to  $12.7\sigma$  for Q4L6 and  $12.9\sigma$  for Q6R2. Adapted under CC BY 4.0 license from [40].

consequently increasing the uncertainty of the measurements. It is, therefore, important that the optics during the aperture measurements remains the same as for the unperturbed machine. The ac-dipole induced  $\beta$  beating is modeled as [19]

$$\frac{\beta_{x,y}^d - \beta_{x,y}}{\beta_{x,y}} = 2\lambda_{x,y}^d \frac{\lambda_{x,y}^d - \cos(2\phi_{x,y}(s) - 2\pi\nu_{x,y})}{1 - (\lambda_{x,y}^d)^2} \quad (3)$$

with

$$\lambda_{x,y}^d = \frac{\sin(\pi\delta_{x,y}^d)}{\sin(2\pi\nu_{x,y} + \pi\delta_{x,y}^d)}, \quad (4)$$

where  $\nu_{x,y}$  is the tune of the machine,  $\phi_{x,y}(s)$  is the phase advance between a given location in the machine and the ac-dipole location,  $\beta_{x,y}^d$  is the ac-dipole driven oscillation  $\beta$  function, and  $\beta_{x,y}$  is the nominal  $\beta$  function without ac-dipole excitation. As the  $\beta$ -beating can be both positive and negative, this can increase the resulting uncertainty.

In Fig. 6, the horizontal  $\beta$ -beating calculated using Eq. (3) as a function of  $\delta_x^d$  for different phase advance values,  $\phi_x(s)$ , is shown for a typical LHC horizontal nominal tune of 0.31. For a value of  $\delta_x^d$  of  $-0.012$ , typically used for optics measurements in the LHC and a nominal tune of 0.31, the maximum  $\beta$  beating expected is 9% for a bottleneck located at  $\phi_x(s) = 90^\circ$ . For a typical aperture measurement of  $10\sigma$ , this introduces an error in the measured aperture of about  $0.45\sigma$ . This error represents the worst-case scenario. For the bottleneck locations found in the experiments presented in this paper, the computed  $\beta$  beating was in all cases lower than 8% at the maximum operation energy and 6% at injection energy. This uncertainty source has been considered in Sec. IV to evaluate the errors associated with the aperture measurements performed with the ac-dipole method.

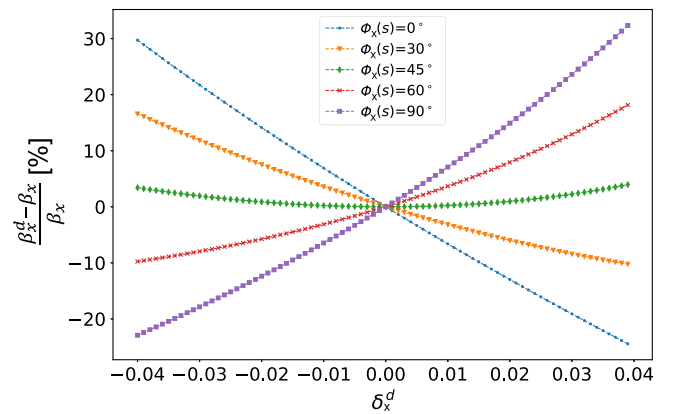


FIG. 6. ac-dipole horizontal  $\beta$ -beating induced effect as a function of  $\delta_x^d$  for different phase advances between the ac dipole and a given location in the ring,  $\phi_x(s)$  for a nominal tune of 0.31.

## B. Tracking simulations

In order to evaluate the feasibility of using ac-dipole excitations for aperture measurements, multiparticle tracking simulations were performed for different horizontal ac-dipole kick amplitudes using the thin lens tracking module of the accelerator design software MAP-X.

The simulations were performed applying the ac-dipole kick in the horizontal plane for the 2018 proton optics with a  $\beta_x^*$  of 25 cm in IR1 and IR5 and a horizontal half-crossing angle of  $145 \mu\text{rad}$ . For the ac-dipole settings, a  $\delta_x^d$  value of  $-0.01$  was chosen based on what was used in the experimental setup in the horizontal measurements performed in 2017 at beam energies of 6500 GeV presented in the next section. The ac-dipole excitation starts after 500 turns and is ramped up for 2000 turns, after which it is kept constant for 6000 turns and finally ramped down for 2000 turns until reaching zero amplitude as can be seen in Fig. 7. A Gaussian beam distribution with a transverse size of  $\pm 3\sigma$  containing 10,000 particles at 6500 GeV was generated with no momentum spread and tracked using the MAD-X tracking module. The losses around the ring have been recorded and analyzed. The initial beam distribution is generated with a horizontal and vertical normalized emittance of  $3.5 \mu\text{m}$ , and a realistic aperture model is used. Note that the measured beam emittance at the LHC shows variations between different fills and even between bunches within the same fill. Furthermore, the relative protection of the aperture does not depend on the absolute beam emittance value, since also the collimator settings depend on the emittance in the same way as the aperture. Therefore, in order to more easily compare different configurations and measurements, depending only on the physical aperture, machine optics, and orbit, and independently of the beam properties, a standardized emittance is typically used for collimator settings and aperture calculations, which is taken as the  $3.5 \mu\text{m}$  LHC design emittance. This is typically larger than the currently achieved beam emittances (to give conservative absolute estimates) and allows easier comparisons between different configurations and years. These simulations were performed for different horizontal ac-dipole kick amplitudes ranging from 1 to 6 mm computed at a location with a horizontal  $\beta$  function of 180 m and for no transverse beam coupling and with a moderate coupling as measured in the LHC during 2018 commissioning (the real and the imaginary parts of the betatron coupling being  $-0.0043$  and  $-0.0017$ , respectively, matched following the procedure in [42]). In the following study, the ac-dipole kick has been applied only to the horizontal plane to illustrate the method. The same procedure applies to vertical aperture measurements.

Figure 7 shows an example of the horizontal turn-by-turn orbit at the beam position monitor BPM.22L1.B1 when applying a 2-mm horizontal ac-dipole excitation amplitude,  $A_x^{\text{ac}}$ , at a location with a  $\beta$  function of 180 m.

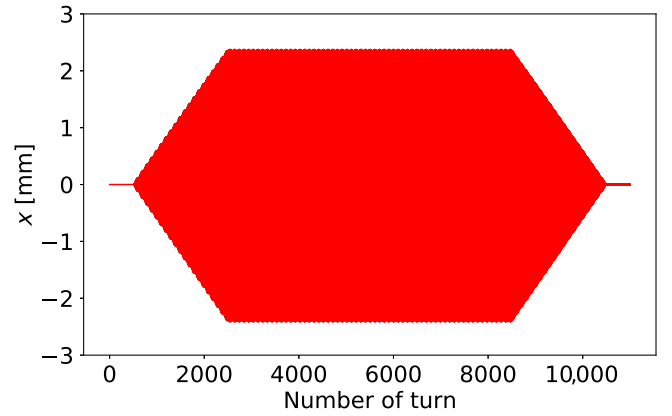


FIG. 7. Simulated excitation pattern of a driven oscillation of about 2 mm at a location with a horizontal  $\beta$  function of 180 m at a frequency  $\nu_x^d$  of 0.299.

In Fig. 8, the summary of the results obtained from these simulations is shown. Losses are observed in one of the triplet magnets, Q2R5, close to the CMS experiment and all the beam is lost for a horizontal ac-dipole kick producing an oscillation of 3 mm (see Fig. 7). For the scenario with a moderate coupling, similar to the one during the 2018 beam commissioning aperture measurements at 6500 GeV, most of the losses still occur in Q2R5 but some losses are now also observed at Q2R1.

In Fig. 9, the horizontal (top) and vertical (middle) closed orbit in IR5 with beam envelopes of 5 and  $10\sigma$  are shown for the 2018 proton colliding optics with  $\beta^* = 25$  cm and a half-crossing angle of  $145 \mu\text{rad}$ . The geometrical aperture model is depicted. In the bottom plot of Fig. 9, the resulting MAD-X aperture calculations in units of  $\sigma$  are shown. Note that this plot takes the minimum over the two planes. For these computations, a closed orbit tolerance of 0.5 mm has been considered, as well as a

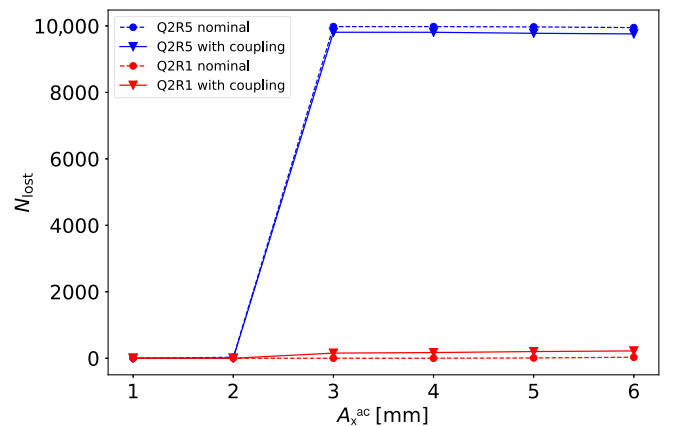


FIG. 8. Particles lost at Q2R5 and Q2R1 magnets as a function of the horizontal ac-dipole kick amplitude for an ideal optics with zero coupling and with the moderate coupling scenario described in this section.

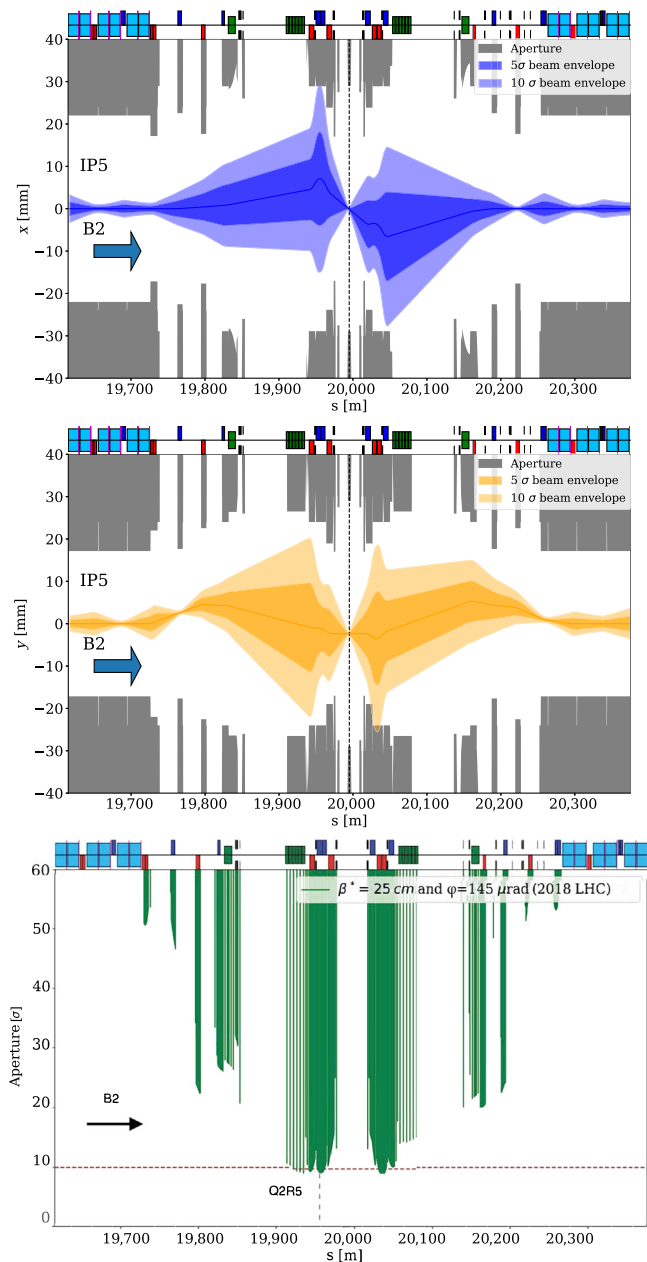


FIG. 9. IR5 horizontal (top) and vertical (middle) closed orbit and 5 and 10 $\sigma$  beam envelopes for the 2018 optics with a  $\beta_{x,y}^*$  of 25 cm and a half-crossing angle of 145  $\mu$ rad. The geometrical aperture model is also plotted and the machine layout is depicted on the top of the plots with dipoles in light blue, focusing quadrupoles in blue, defocusing quadrupoles in red, sextupoles in green, and collimators in black. The bottom plot shows an example of the aperture calculated with the MAD-X algorithm in units of  $\sigma$ . A red line was added for reference at 10 $\sigma$ .

relative momentum offset of  $2 \times 10^{-4}$ , a 5%  $\beta$ -beating, and a fractional parasitic dispersion from the arc of 10%, as in [7]. For the calculation of the beam size, the nominal normalized emittance of 3.5  $\mu$ m has been used. Combining the results from the three figures, one can determine that the minimum aperture in the horizontal plane corresponds to

the aperture at the Q2R5 magnet. This result is in agreement with the tracking results summarized in Fig. 8, in which the ac dipole was used to increase the amplitude of the particle oscillation around the closed orbit to identify the bottleneck of the machine where the particles are lost.

#### IV. EXPERIMENTAL RESULTS

In this section, the experimental results from different campaigns carried out in 2017 and 2018 are presented. Three experiments were performed at the LHC injection energy of 450 GeV and optics, in the horizontal plane for both beams, and one experiment was performed at the maximum operating energy of 6500 GeV, for both planes and beams for a low- $\beta$  optics ( $\beta_{x,y}^* = 30$  cm) configuration.

##### A. Measurements at 450 GeV and injection optics

In 2017, the first two dedicated experiments on injection optics and energy were performed on September 15 (MD1) and November 29 (MD2) to investigate the feasibility of using ac-dipole excitations for *global* aperture measurements using a well-measured machine configuration. A first analysis of the results obtained was presented in [40]. The ac-dipole settings and beam parameters deployed during these tests are summarized in Table II.

Before starting the aperture measurements in MD1, emittance measurements were performed with a wire scanner in order to verify that the emittance is preserved after applying kicks with the ac dipole. The horizontal kicks were varied in the range of 0.9–5.8 mm. The measured horizontal emittances are summarized in Table III with an associated error of about 6% from Ref. [43]. The observed variation between measurements is within the associated error of 0.2  $\mu$ m rad, validating the main advantages of the ac-dipole method with respect to the transverse damper one.

Then, measurements were first performed using the ac-dipole method and afterward with the transverse damper method. A primary collimator in IR7 was used as reference collimator for the aperture scans with the loss

TABLE II. ac dipole and beam settings for the aperture measurements performed at the injection energy of 450 GeV and optics. The horizontal and vertical kicks are computed at a location with a  $\beta$  function of about 180 m.

Parameter	Beam 1	Beam 1	Beam 2
MD	1	2	3
Plane	H	H	H
Horizontal driven tune, $\delta_x^d$	-0.012	-0.012	$\pm 0.012$
Vertical driven tune, $\delta_y^d$	+0.01	+0.01	$\pm 0.01$
Horizontal kick (mm)	9	11	10
Vertical kick (mm)	1.3	2	1.2
Energy, $E$ (GeV)	450	450	450
Chromaticity, $\xi_{x,y}$	3	3	3, 15

TABLE III. Horizontal emittance measurements performed with the LHC wire scanner in the 2017 MD1.

Horizontal kick (mm)	Horizontal emittance ( $\mu\text{m rad}$ )
0.9	$3.9 \pm 0.2$
2.2	$3.6 \pm 0.2$
2.7	$3.8 \pm 0.2$
3.1	$3.8 \pm 0.2$
4.1	$3.8 \pm 0.2$
5.8	$3.8 \pm 0.2$

rates analyzed, as described in Sec. III. An example of one of the collimator scans performed during MD1 was already shown in Fig. 5 in the form of losses at the reference collimator (black) and at the bottlenecks (red and blue), as a function of the primary collimator half-gap in units of  $\sigma$ . Note that during the scan, at each collimator setting, a new excitation of the bunch is performed until losses are observed at the collimator or at the bottleneck location. Losses were observed at the same time in two different magnets, one in IR2 and the other in IR6, indicating that we have a very similar aperture value at these two locations. In this analysis, we define the measured aperture of the bottleneck as the collimator half-aperture before exposing the bottleneck, plus half of the collimator scan step. The error associated with each aperture value obtained with the ac-dipole method is computed as the square root of the sum of the squares of the relative measurement errors given by half of the step of the scan ( $0.25\sigma$ ) and the ac-dipole induced  $\beta$  beating. The last contribution has been computed at the reference collimator and at the bottleneck location using Eq. (3). The total  $\beta$ -beating induced contribution is computed as a difference between the two locations, such that for two locations with opposite sign of  $\beta$  beating, the contributions are summed and for two locations with the same sign of  $\beta$  beating, the contributions are subtracted. The error associated with the measurements based on the transverse damper technique is directly given by half of the collimator scan step as explained in [4].

A summary of all the measurements performed during these experiments is shown in Fig. 10. The results obtained with the two methods are compatible with the error associated with each method. The major difference between the ac dipole and the beam transverse damper technique is found in the aperture of the bottleneck at Q6L6 during MD1, showing a difference of  $0.5\sigma$ . This could be partially explained by a beam orbit drift observed in IR6 of about  $100 \mu\text{m}$  corresponding to  $0.1\sigma$ . In addition, losses were also observed on Beam 2 which was being used for another experiment at the same time as the aperture measurements on Beam 1 were performed. These losses could also reach the Beam 1 BLMs in IR6 affecting the aperture measurements. During MD2, the orbit and losses generated from the other beam were better controlled and a better agreement was found in the results as can be seen in Fig. 10.

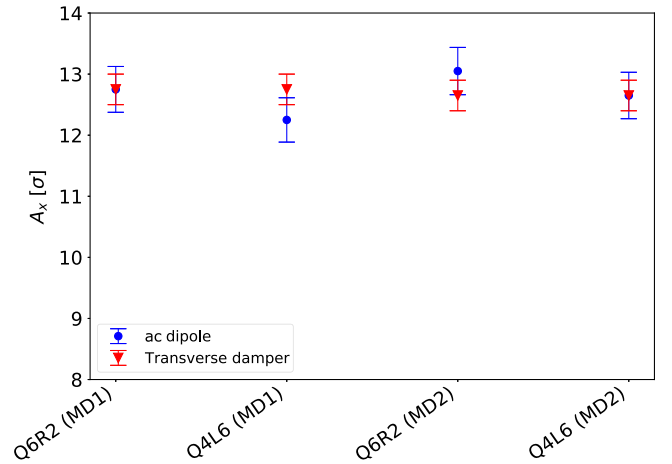


FIG. 10. Summary of the horizontal aperture measurements performed for beam 1 at injection energy and optics with the ac dipole (blue) and the transverse damper (red) methods during MD1 and MD2.

In the experiment performed in 2018 (MD3), instead of measuring the *global* aperture bottleneck of the machine, the horizontal tertiary collimator in IR5 was closed to an aperture of  $10\sigma$ , aligned, and used to mimic the aperture restriction to be measured. Again, a primary collimator in IR7 was used as a reference collimator for the aperture scans. In these measurements the effect on the results induced by a change in the ac-dipole driving tune and beam chromaticity was investigated on Beam 2. The ac-dipole settings and beam parameters deployed during these measurements are summarized in Table II.

Measurements were performed with the ac dipole with two different ac-dipole driving tunes and for two different chromaticities as well as with the transverse damper. In all cases and with both methods the same bottleneck location was identified (the tertiary collimator in IR5). A summary

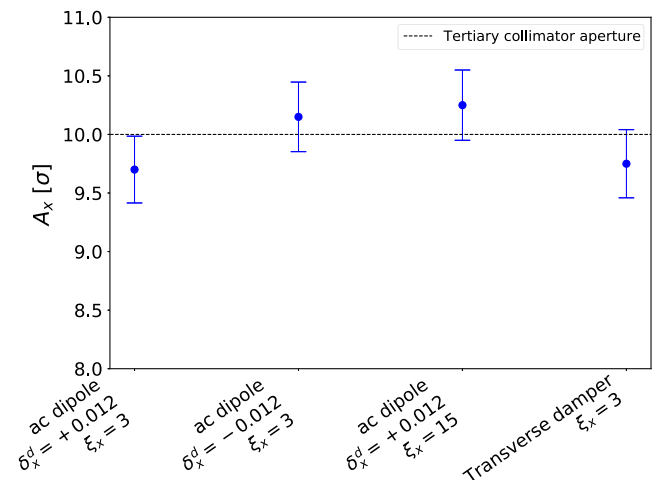


FIG. 11. Summary of horizontal aperture measurements performed in MD3 for beam 2 at injection optics and energy for different ac-dipole settings and beam chromaticity.

TABLE IV. ac-dipole and beam parameters for the measurements at the maximum operation energy of 6500 GeV. The horizontal and vertical kicks are calculated at a location with a  $\beta$  function of about 180 m.

Parameter	Beam 1	Beam 1	Beam 2	Beam 2
Plane	H	V	H	V
Horizontal driven tune, $\delta_x^d$	-0.01	-0.01	-0.01	-0.01
Vertical driven tune, $\delta_y^d$	0.012	0.012	0.012	0.012
Horizontal kick (mm)	1.5	1.4	2.3	1.6
Vertical kick (mm)	0.9	2.4	0.9	2.2
Energy, $E$ (GeV)	6500	6500	6500	6500
Chromaticity, $\xi_{x,y}$	3	3	3	3

of the aperture values found is shown in Fig. 11, with the associated errors computed as described for MD1 and MD2. The measured aperture values are compatible within  $0.3\sigma$  in all cases.

The effect of the ac-dipole driven tune in the ranges studied [44], summarized in Table II, is within the method uncertainty. Concerning the impact of the beam chromaticity, a very pessimistic scenario was chosen in which the value of the chromaticity was set to 15 in comparison to the value of 3 typically used in operation. The measurement result in such a scenario is also compatible with the expectation and the difference with respect to a configuration with a chromaticity value of 3 is about 5%.

### B. Measurements at 6500 GeV and low $\beta$ optics

The new ac-dipole method for aperture measurements was also tested at the maximum 2017 LHC operation energy of 6500 GeV. The *global* aperture measurements were performed for beam 1 and beam 2 in both the

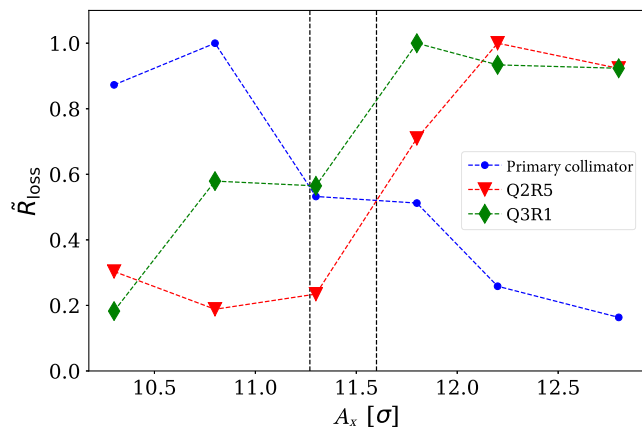


FIG. 12. Beam 2 horizontal aperture measurements for the 2017 top energy optics with  $\beta^* = 30$  cm. The normalized BLM signals at the primary collimator (blue) and at the bottleneck in IR5 (red) and IR1 (green) are shown as a function of the primary collimator half-gap. The corresponding half-gap at which the collimator and the bottleneck curves cross is indicated with dash black lines.

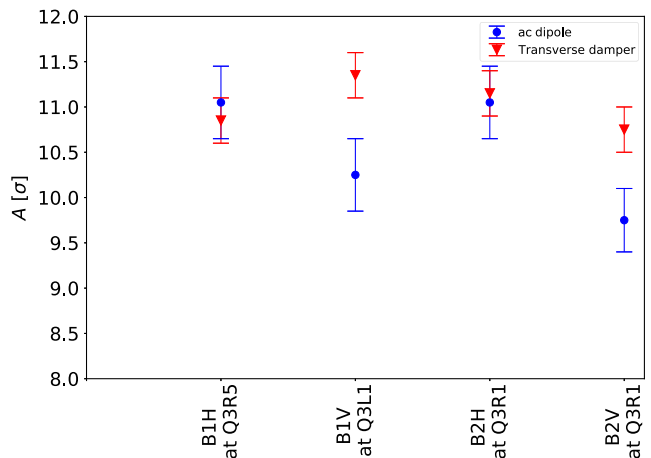


FIG. 13. Comparison of the ac dipole and transverse damper measured apertures for beam 1 and beam 2 in both planes from the 2017 campaign at top energy with colliding beam optics ( $\beta^* = 30$  cm).

horizontal and the vertical planes for the colliding beams optics with  $\beta_{x,y}^* = 30$  cm. The ac-dipole and the beam parameters used are summarized in Table IV. The primary collimators used in IR7 were used for the aperture scans.

For all beams and planes, the bottlenecks were found in the triplets in IR1 and IR5 as measured in the 2017 beam commissioning with the transverse damper method [45].

In Fig. 12, an example of these measurements is shown for Beam 2 in the horizontal plane. The normalized measured BLM signals at the primary collimator (in blue), used as a reference collimator for the scan, and at the bottlenecks in IR5 and IR1 (in red and green, respectively) are shown as a function of the collimator half-gap in units of  $\sigma$ . The half-gap at which the collimator and the bottleneck curves cross, indicated with dash black lines, corresponds to the aperture bottleneck in units of  $\sigma$ .

A summary of the ac dipole results in comparison with the transverse damper method is shown in Fig. 13. The same aperture and error calculation procedure as used to analyze the injection energy data have been used. Note that the aperture values in Ref. [45] are directly the values of the

TABLE V. ac dipole and beam parameters for the measurements at 6500 GeV and  $\beta_{x,y}^* = 25$  cm in 2018. The horizontal and the vertical kicks are computed at a location with a  $\beta$  function of about 180 m.

Parameter	Beam 2	Beam 2
Plane	H	V
Horizontal driven tune, $\delta_x^d$	0.012	0.012
Vertical driven tune, $\delta_y^d$	-0.015	-0.015
Horizontal kick (mm)	2.5	0.8
Vertical kick (mm)	0.9	2.4
Energy, $E$ (GeV)	6500	6500
Chromaticity, $\xi_{x,y}$	3	3

TABLE VI. Beam 2 vertical aperture measurement results for both the transverse damper and the ac-dipole method at 6500 GeV beam energy during the 2018 LHC commissioning.

Method	Collimator step ( $\sigma$ )	Interpolated aperture ( $\sigma$ )	Bottleneck
ac dipole	10–11	$10.2 \pm 0.4$	Q3R1
Transverse damper	10–10.5	$10.3 \pm 0.25$	Q3R1

reference collimator before exposing the bottleneck and not the interpolated values illustrated in Fig. 12.

Both methods agree well on the localization of the bottlenecks for both beams and planes. The measured apertures are compatible, within  $0.4\sigma$  in the horizontal plane and within  $1\sigma$  in the vertical plane [46]. With the ac-dipole method, kicks were also applied in the plane orthogonal to the measurement as can be seen in Table IV. If small enough, they are expected to have a negligible impact on the results. However, the sensitivity of the impact of these kicks depends on the optics at the bottleneck and on the mechanical shape of the aperture bottleneck. The origin of the larger differences observed in the vertical plane could be explained by the nonoptimized ac-dipole settings chosen for the vertical measurements. More details are given in the next section. In future measurements, it is important to reduce the kick on the plane not being measured to 0 to avoid this problem.

In order to validate the technique in the vertical plane, a quick test was performed at 6500 GeV beam energy with both the transverse damper and the ac-dipole method, during the 2018 LHC commissioning for beam 2. These measurements were performed for the beam optics with  $\beta_{x,y}^* = 25$  cm using the tertiary collimators in IR1 and IR5 as reference and the ac dipole setup summarized in Table V.

The measurements performed in the vertical plane from the two techniques agreed well on the bottleneck localization and the measured apertures are compatible within  $0.4\sigma$  as summarized in Table VI.

In this quick test, the horizontal plane was also measured for completeness but losses were observed at an unexpected location. Due to lack of time, it was not possible to investigate the origin with beam and the off-line analysis could not explain the observations. More details are given in the discussion section.

## V. DISCUSSION

All aperture measurements performed with the ac-dipole method for both beams and planes at injection optics and energy are compatible with the transverse damper method within  $0.3\sigma$ . These results are the first proof-of-principle of using ac dipoles for nondestructive aperture measurements.

The results at the Run 2 LHC maximum energy and low- $\beta$  optics are promising. In the first dedicated experiment, an agreement between methods within  $0.4\sigma$  was obtained in the horizontal plane. In the vertical plane, the agreement was within  $1\sigma$ .

The larger discrepancy observed in the vertical plane could be explained by the impact of the kick being applied on the nonmeasuring plane. The geometrical aperture for the particular case of Q3R5 is illustrated in Fig. 14.

Most of the LHC quadrupoles have this geometrical shape but it can be rotated by  $90^\circ$ . As can be seen in Fig. 14 in one plane, the aperture has a rectangular section while on the other plane, the section is all elliptical. From the geometrical shape, one can see that if the aperture restriction is found on the plane with the rectangular section, we expect no effect from a kick on the nonmeasuring plane, and no hit on the curved section unless combined with possible mechanical misalignment values of more than 17 mm. However, in the other plane, the section is all curved and we are more sensitive to a kick in the nonmeasuring plane. The impact on the measurements of the kick applied on the orthogonal to the measurement plane increases as we move far from the center. For this particular example, a displacement in the vertical plane of 10 mm corresponds to a loss in the horizontal aperture of  $1\sigma$ .

Initially, one of the main motivations to develop the ac-dipole technique was to measure aperture and optics together. For optics measurements, kicks are applied in both planes at the same time. The nonzero kick in the plane, orthogonal to the one being measured is a leftover of the initial intention. Based on the experience at injection, the applied kicks on the nonmeasuring plane used were

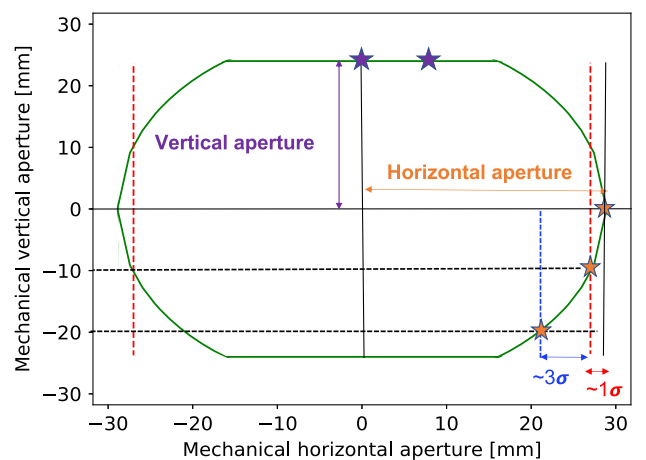


FIG. 14. Q3R5 geometrical aperture. The added star points and lines at different impacting points at the geometrical aperture illustrate the effect of a kick on the orthogonal to the measurement plane for different aperture shapes.

TABLE VII. Summary of the main parameters used and computed in the analysis of the impact of the ac-dipole kick on the nonmeasuring plane for the 2017 and the 2018 data.

Energy (GeV)	Beam	Plane	Horizontal kick (mm)	Vertical kick (mm)	Bottleneck	Bottleneck shape	Kick at bottleneck in the nonmeasurement plane (mm)	Aperture loss ( $\sigma$ )
450	1	H	9	1.3	Q6R2	Elliptical in horizontal	1.7	0.2
450	1	H	11	2	Q4L6	Rectangular in horizontal	4	No effect
6500	1	H	1.5	0.9	Q3R5	Elliptical in horizontal	4.4	0.2
6500	1	V	1.4	2.4	Q3L1	Elliptical in vertical	8.2	0.7
6500	2	H	2.3	0.9	Q3R1	Rectangular in horizontal	10.6	No effect
6500	2	V	1.6	2.2	Q3R1	Elliptical in vertical	7.5	0.5
6500	2	V	0.8	2.4	Q3R1	Elliptical in vertical	4.5	0.2

expected to have a negligible impact. However, as was investigated after the 2017 set of measurements at top energy, the sensitivity of the kick in the nonmeasuring plane is subject to the optics and aperture shape at the bottleneck. For the 2017 measurements, the nonoptimized ac-dipole settings and the optics at the vertical bottlenecks made the impact to be more significant than for the horizontal measurements at top energy and all measurements at injection energy.

In order to validate our hypothesis, we performed a quick measurement in 2018 for Beam 2 in the vertical plane. For this test, the kick in the orthogonal to the measurement plane was decreased by a factor of 2 and the methods agreed within  $0.4\sigma$ .

Table VII summarizes the main parameters considered and computed to analyze the impact of the ac-dipole kick on the nonmeasuring plane for the 2017 and 2018 data. Table VII includes the beam energy, the beam and plane being measured, the ac-dipole horizontal and vertical kicks applied in each measurement, the bottleneck location, and shape on the limiting plane, the displacement computed based on the optics at the bottleneck location induced by the kick applied on the plane not being measured and the corresponding aperture loss for an ideal machine.

As can be seen in Table VII in the last column, for most of the measurements performed, the expected impact from the kick in the nonmeasuring plane is smaller than the associated error to the measurements within  $0.3$ – $0.4\sigma$ . For these cases, an agreement within the associated error is found between methods. The only two cases in which the expected aperture loss is above the associated error to the methods correspond to the measurements in the vertical plane from 2017 at top energy. For these two cases, the ac-dipole method measures a smaller aperture up to  $1\sigma$  than the transverse damper method. The 2018 quick test performed at top energy in the vertical plane demonstrated that reducing the kick on the horizontal plane by a factor of 2 reduces the impact of this kick to the precision of the method level ( $0.4\sigma$ ). Note that for these calculations, an ideal machine has been considered. Despite that, these results indicate the possible origin of the discrepancy observed and highlight the need to void the kick in the nonmeasuring plane in future measurements.

For completeness, as introduced in the previous section of the 2018 quick test, the horizontal plane was also measured. However, the highest loss spike in the horizontal plane using the ac-dipole method was observed at the Q5R5 quadrupole throughout all the reference collimator scans from  $9$  to  $12\sigma$ . Because there was no dedicated time for the measurements, this could not be investigated further with beam and going to smaller reference collimator aperture values and had to be investigated off-line. The bottleneck is expected at the triplet magnets in IR5 or IR1, and no losses were observed at Q5R5 during the aperture measurements performed with the transverse damper method. Off-line analysis was performed and the possible impact of the measured transverse beam coupling was explored in tracking simulations which results are presented in Sec. III as the beam coupling was discovered to be higher than typically used after the optics corrections. However, no change in the bottleneck location and no significant impact on the losses is expected due to the transverse beam coupling value studied, as can be seen in Fig. 8. The possible origin of the observed losses in Q5R5 due to off-momentum beam was also investigated but simulations do not reveal the Q5R5 as a possible bottleneck in such scenario. Due to the lack of data, it was not possible to check if there was off-momentum beam circulating in the machine during the measurements. The beam orbit was also investigated but the observed orbit shift at the location of the losses could not explain the observations. Only this quick test made in nonideal conditions gave us an unexpected observation which origin is not possible to investigate further with the available data. Experimental efforts will continue during Run 3 in order to answer this open point and optimize the new method for use during beam commissioning periods.

## VI. CONCLUSIONS

Aperture measurements are crucial for the safe operation of the LHC and to push its luminosity performance. A new aperture measurement method based on the use of ac-dipole excitations has been explored for the first time. The time required by the ac-dipole method is slightly longer than for

the standard LHC method based on the use of a transverse damper by a few minutes due to the time needed by the ac dipole to cooldown after each excitation. However, the method is nondestructive and can be combined with other commissioning activities, reducing the number of fills, bunches, and injections in each fill, for an overall gain in efficiency. In addition, it can be combined with optics measurements such as amplitude detuning and resonance driving term measurements to probe the aperture for the configuration directly during these measurements, ensuring that the optics can be explored safely using the maximum oscillation amplitude increasing the precision of those measurements.

The new method has been benchmarked against the destructive transverse damper method used in the LHC as the standard approach for aperture measurements. In general, good agreement has been found between the identified location of the bottlenecks between methods. The measured aperture values in units of  $\sigma$  have been found to be compatible with the measurements performed with the transverse damper method, within the associated errors, with the exception of two cases at top energy in the vertical plane where nonideal setup conditions were identified in the analysis and the origin of the observed discrepancy was understood. From these measurements, we could conclude that the kick on the plane not being measured has to be minimized or setup to 0 in order to not interfere with the measurements. The sensitivity of the measured aperture to different ac-dipole and machine parameter configurations was also studied in the ranges of interest for the LHC and found to be negligible. Only for one horizontal aperture, measurement performed at the lowest operational  $\beta^*$  of 25 cm in a quick test the bottleneck was identified in a different location. Experimental efforts will continue during Run 3 in order to answer this open point.

The experimental tests presented in this paper demonstrate the feasibility of using the nondestructive ac-dipole method, which could be used to further optimize the LHC commissioning activities during the upcoming LHC runs, as well as in any other synchrotron to provide an accurate measurement of the aperture and bottlenecks of the machine.

### ACKNOWLEDGMENTS

The authors would like to thank colleagues in the collimation and optics teams for valuable discussions as well as the LHC operation team, in particular to B. Salvachua, for their help in the acquisition of the data analyzed in this paper.

- 
- [1] O. S. Brüning *et al.*, LHC design report v.1: The LHC main ring, Report No. CERN-2004-003-V1, 2004.
  - [2] R. Bruce, R. W. Assmann, and S. Redaelli, Calculations of safe collimator settings and  $\beta^*$  at the CERN Large Hadron Collider, *Phys. Rev. ST Accel. Beams* **18**, 061001 (2015).

- [3] R. Bruce, C. Bracco, R. D. Maria, M. Giovannozzi, A. Mereghetti, D. Mirarchi, S. Redaelli, E. Quaranta, and B. Salvachua, Reaching record-low  $\beta^*$  at the CERN Large Hadron Collider using a novel scheme of collimator settings and optics, *Nucl. Instrum. Methods Phys. Res., Sect. A* **848**, 19 (2017).
- [4] N. Fuster-Martínez, R. W. Assmann, R. Bruce, M. Giovannozzi, P. Hermes, A. Mereghetti, S. Redaelli, and J. Wenninger, Beam-based aperture measurements with movable collimator jaws as performance booster of the CERN Large Hadron Collider, *Eur. Phys. J. Plus* **137**, 305 (2022).
- [5] J. Jeanneret and T. Risselada, Geometrical aperture in LHC at injection, LHC Project Note 66, CERN, 1996.
- [6] J. Jeanneret and R. Ostojic, Geometrical acceptance in LHC version 5.0, LHC Project Note 111, CERN, 1997.
- [7] R. Bruce, R. de Maria, S. Fartoukh, M. Giovannozzi, S. Redaelli, R. Tomás, and J. Wenninger, Parameters for HL-LHC aperture calculations, CERN Report No. CERN-ACC-2014-0044, 2014.
- [8] J. M. Jowett *et al.*, Overview of ion runs during Run 2, in *Proceedings of the 9th LHC Operations Evian Workshop, Evian, France* (2019).
- [9] R. Bruce, M. Jebramcik, J. Jowett, T. Mertens, and M. Schaumann, Performance and luminosity models for heavy-ion operation at the CERN Large Hadron Collider, *Eur. Phys. J. Plus* **136**, 745 (2021).
- [10] E. Holzer *et al.*, Beam loss monitoring system for the LHC, *IEEE Nucl. Sci. Symp. Conf. Rec.* **2**, 1052 (2005).
- [11] E. B. Holzer *et al.*, Development, production and testing of 4500 beam loss monitors, in *Proceedings of the 11th European Particle Accelerator Conference, Genoa, 2008* (EPS-AG, Genoa, Italy, 2008), p. 1134.
- [12] R. Bruce, P. D. Hermes, H. Garcia, R. Kwee-Hinzmann, A. Mereghetti, D. Mirarchi, S. Redaelli, P. Skowronski, G. Valentino, and A. Valloni, IR aperture measurement at  $\beta^* = 40$  cm, Report No. CERN-ACC-NOTE-2015-0037, 2015.
- [13] R. Tomás, M. Aiba, A. Franchi, and U. Iriso, Review of linear optics measurement and correction for charged particle accelerators, *Phys. Rev. Accel. Beams* **20**, 054801 (2017).
- [14] J. Serrano and M. Cattin, The LHC AC-dipole system: An introduction, Report No. CERN-BE-Note-2010-014, 2010.
- [15] R. Tomás, S. Fartoukh, and J. Serrano, Reliable operation of the AC dipole in the LHC, Report No. LHC-PROJECT-Report-1095, 2008, p. 4.
- [16] T. Persson *et al.*, LHC optics commissioning: A journey towards 1% optics control, *Phys. Rev. Accel. Beams* **20**, 061002 (2017).
- [17] F. S. Carlier, R. Tomás, E. H. Maclean, and T. Persson, First experimental demonstration of forced dynamic aperture measurements with LHC ac dipoles, *Phys. Rev. Accel. Beams* **22**, 031002 (2019).
- [18] M. Bai *et al.*, Overcoming Intrinsic Spin Resonances with an rf Dipole, *Phys. Rev. Lett.* **80**, 4673 (1998).
- [19] R. Miyamoto, S. E. Kopp, A. Jansson, and M. J. Syphers, Parametrization of the driven betatron oscillation, *Phys. Rev. ST Accel. Beams* **11**, 084002 (2008).

- [20] R. Miyamoto *et al.*, Tevatron AC-dipole system, in *Proceedings of the 22nd Particle Accelerator Conference, PAC-2007, Albuquerque, NM* (IEEE, New York, 2007).
- [21] R. Tomás, Normal form of particle motion under the influence of an ac dipole, *Phys. Rev. ST Accel. Beams* **5**, 054001 (2002).
- [22] S. White, E. Maclean, and R. Tomás, Direct amplitude detuning measurement with ac dipole, *Phys. Rev. ST Accel. Beams* **16**, 071002 (2013).
- [23] E. Maclean *et al.*, New approach to LHC optics commissioning for the nonlinear era, *Phys. Rev. Accel. Beams* **22**, 061004 (2019).
- [24] F. S. Carlier, A nonlinear future—measurements and corrections of nonlinear beam dynamics using forced transverse oscillations, Ph.D. thesis, Amsterdam University, 2020.
- [25] R. Tomás, X. Buffat, S. White, J. Barranco, P. Gonçalves Jorge, and T. Pieloni, Beam-beam amplitude detuning with forced oscillations, *Phys. Rev. Accel. Beams* **20**, 101002 (2017).
- [26] N. Biancacci and R. Tomás, Using ac dipoles to localize sources of beam coupling impedance, *Phys. Rev. Accel. Beams* **19**, 054001 (2016).
- [27] R. Tomás, Cooling an annular beam with resonances, in *Proceedings of Non-Linear Beam Dynamics WG Meeting*, (2020), <https://indico.cern.ch/event/966240/>.
- [28] F. Caponni, Latest results on cooling an annular beam distribution, in *Proceedings of Non-Linear Beam Dynamics WG Meeting* (2021), <https://indico.cern.ch/event/1014203/>.
- [29] A. Franchi, Recent measurements of linear and nonlinear optics at the ESRF storage ring, in *Proceedings of the 7th Low-Emittance Rings Workshop* (2018), <https://indico.cern.ch/event/671745/contributions/2788842/>.
- [30] I. Agapov *et al.*, Linear and nonlinear optics measurements with multiturn data at PETRA III, CERN Technical Report No. CERN-ACC-2017-258, 2017.
- [31] L. Malina, AC dipole experience in PETRA, in *Proceedings of FCC-ee Tuning Meeting* (2022), <https://indico.cern.ch/event/1138028/>.
- [32] J. Keintzel, AC dipole experience in SuperKEKB, in *Proceedings of FCC-ee Tuning Meeting* (2022), <https://indico.cern.ch/event/1138028/>.
- [33] U. Iriso, (private communication).
- [34] R. Bruce *et al.*, Sources of machine-induced background in the ATLAS and CMS detectors at the CERN Large Hadron Collider, *Nucl. Instrum. Methods Phys. Res., Sect. A* **729**, 825 (2013).
- [35] R. Bruce, M. Huhtinen, A. Manousos, F. Cerutti, L. Esposito, R. Kwee-Hinzmann, A. Lechner, A. Mereghetti, D. Mirarchi, S. Redaelli, and B. Salvachua, Collimation-induced experimental background studies at the CERN Large Hadron Collider, *Phys. Rev. Accel. Beams* **22**, 021004 (2019).
- [36] R. Assmann, B. Goddard, E. Vossenberg, and E. Weisse, The consequences of abnormal beam dump actions on the LHC collimation system, LHC Project Note 293, CERN, 1996.
- [37] R. Schmidt, R. Assmann, E. Carlier, B. Dehning, R. Denz, B. Goddard, E. B. Holzer, V. Kain, B. Puccio, B. Todd, J. Uythoven, J. Wenninger, and M. Zerlauth, Protection of the CERN Large Hadron Collider, *New J. Phys.* **8**, 290 (2006).
- [38] E. Quaranta, Investigation of collimator materials for the High Luminosity Large Hadron Collider, Ph.D. thesis, Politecnico di Milano, 2017.
- [39] R. Tomás, Adiabaticity of the ramping process of an ac dipole, *Phys. Rev. ST Accel. Beams* **8**, 024401 (2005).
- [40] N. Fuster-Martínez, R. Bruce, J. Dilly, E. Maclean, L. Nevay, T. Persson, S. Redaelli, and R. Tomás, Aperture measurements with ac dipole at the Large Hadron Collider, in *Proceedings of the International Particle Accelerator Conference 2018, Vancouver, BC, Canada* (JACoW, Geneva, Switzerland, 2018), MOPMF048, p. 4.
- [41] F. S. Carlier and R. Tomás and E. Maclean and T. Persson, First experimental demonstration of forced dynamic aperture measurements with LHC ac dipoles, *Phys. Rev. Accel. Beams* **22**, 031002 (2019).
- [42] R. Tomás, Optimizing the global coupling knobs for the LHC, Report No. CERN-ATS-Note-2012-019 MD, 2012.
- [43] G. Trad, personal communication.
- [44] N. Fuster-Martínez *et al.*, MD4506: Aperture measurements with AC-dipole, in Proceedings of Oral presentation at the LHC Collimation Working Group (2018), [https://indico.cern.ch/event/674171/contributions/2758222/attachments/1545493/2425666/AC\\_dipole\\_MD\\_WC\\_.pdf](https://indico.cern.ch/event/674171/contributions/2758222/attachments/1545493/2425666/AC_dipole_MD_WC_.pdf).
- [45] R. B. *et al.*, Review of LHC Run 2 machine configurations, in *Proceedings of the 9th Evian Workshop, Evian Les Bains, France*, (2019), <https://inspirehep.net/files/3f70757c713d4f8254a581989269f979>.
- [46] N. Fuster-Martínez *et al.*, Aperture measurements with AC-dipole, in Proceedings of OMC-OP Workshop (2019), <https://indico.cern.ch/event/828284/contributions/3473471/>.